NIH Public Access
Author Manuscript
Chem Biol. Author manuscript; available in PMC 2010 May 29.

Published in final edited form as:
Chem Biol. 2009 May 29; 16(5): 531–539. doi:10.1016/j.chembiol.2009.03.006.

Mutational Separation of Aminoacylation and Cytokine Activities of Human Tyrosyl-tRNA Synthetase

Mili Kapoor, **Francella J. Otero**, **Bonnie M. Slike**, **Karla L. Ewalt**, and **Xiang-Lei Yang***
Departments of Molecular Biology and Chemistry and The Skaggs Institute for Chemical Biology, The Scripps Research Institute, 10550 North Torrey Pines Road, La Jolla, California 92037, USA

SUMMARY

Aminoacyl-tRNA synthetases are known for catalysis of aminoacylation. Significantly, some mammalian synthetases developed cytokine functions possibly linked to disease-causing mutations in tRNA synthetases. Not understood is how epitopes for cytokine signaling were introduced into catalytic scaffolds without disturbing aminoacylation. Here we investigate human tyrosyl-tRNA synthetase, where a catalytic-domain surface helix—next to the active site—was recruited for IL-8-like cytokine signaling. Taking advantage of our high-resolution structure, the reciprocal impact of rational mutations designed to disrupt aminoacylation or cytokine signaling was investigated with multiple assays. The collective analysis demonstrated a protective fine–structure separation of aminoacylation from cytokine activities within the conserved catalytic domain. As a consequence, disease-causing mutations affecting cell signaling can arise without disturbing aminoacylation. These results with TyrRS also predict the previously unknown binding conformation of IL-8-like CXC cytokines.

Introduction

Aminoacyl-tRNA synthetases (AARS) catalyze aminoacylation of tRNA, specifically pairing amino acids with their cognate anticodons on tRNA, thereby establishing the rules of the genetic code. These enzymes are thought to have arisen during the transition from the ‘RNA world’ and their long evolution led to myriad structural and functional adaptations. For example, specific enzymes developed editing activities during evolution to increase specificity and selectivity of aminoacylation. In addition, idiosyncratic adaptations led to the development of expanded cellular activities that link aminoacylation with the broad systems biology of higher eukaryotes (Antonellis et al., 2008; Lee et al., 2004; Martinis et al., 1999; Park et al., 2005, 2008). It is these expanded functions that are thought to explain why heritable mutations in genes for specific synthetases are causally connected to diseases (Antonellis et al., 2008; Park et al., 2008). Examples include mutations in glycyl-, tyrosyl- and aspartyl-tRNA synthetases, where either protein synthesis or the respective aminoacylation activity is unimpaired by the disease-causing mutation (Antonellis et al., 2006; Jordanova et al., 2006; Nangle et al., 2007; Scheper et al., 2007; Seburn et al., 2006). Not understood is how a tRNA synthetase structural scaffold was expropriated for another activity, and done so in a way that does not disrupt aminoacylation. To better understand this question, we investigated human

*Corresponding author: E-mail: xlyang@scripps.edu, Phone: (858) 784-8976, Fax: (858) 784-7250.

Publisher's Disclaimer: This is a PDF file of an unedited manuscript that has been accepted for publication. As a service to our customers we are providing this early version of the manuscript. The manuscript will undergo copyediting, typesetting, and review of the resulting proof before it is published in its final citable form. Please note that during the production process errors may be discovered which could affect the content, and all legal disclaimers that apply to the journal pertain.

NIH-PA Author Manuscript
NIH-PA Author Manuscript
NIH-PA Author Manuscript

NIH-PA Author Manuscript

NIH-PA Author Manuscript

NIH-PA Author Manuscript

TyrRS as an example. We chose this synthetase because of the availability of our high resolution structure, and of at least three assays that can monitor its cytokine activity.

Several examples of diversification of the functional repertoire of tRNA synthetases abound in literature. Thus, the unique fused glutamyl-prolyl-tRNA synthetase regulates translational silencing of ceruloplasmin, a multifunctional oxidase involved in inflammation responses in mammals (Sampath et al., 2004). Glutaminyl-tRNA synthetase has an anti-apoptotic role through its inhibition of the apoptosis signal regulating kinase-1 in a glutamine-dependent manner (Ko et al., 2001). Motif 1 of human lysyl-tRNA synthetase interacts with the C-terminal capsid region of the human immunodeficiency virus (HIV) gag protein and promotes packaging of the HIV virion together with its $tRNA^{Lys}$ primer for reverse transcription (Javanbakht et al., 2003). Histidyl-tRNA synthetase and asparaginyl-tRNA synthetase activate chemokine receptors on T-lymphocytes and immature dendritic cells (Howard et al., 2002). And a potent inhibitor of angiogenesis is found in human tryptophanyl-tRNA synthetase, whose expression is regulated by interferon-γ (Wakasugi et al., 2002a).

TyrRS developed cell-signaling activities that are regulated by its appended C-terminal domain (C-domain) (Figure 1A). Native, full-length TyrRS has no known cytokine activity. Proteolytic removal of the C-domain from TyrRS activates its cytokine function (Wakasugi and Schimmel, 1999a, 1999b). The N-terminal fragment, mini-TyrRS, specifically stimulates migration of endothelial cells and polymorphonuclear leukocytes (PMNs), and is pro-angiogenic in cell based assays (Wakasugi and Schimmel, 1999a; Wakasugi et al., 2002b) and in an ischemic mouse ear angiogenesis model (Cheng et al., 2008). Mini-TyrRS is exported from endothelial cells after treatment with tumor necrosis factor-α and activates an array of angiogenesis signal transduction pathways (Greenberg et al., 2008). The C-domain of TyrRS is unique to segmented animals, is distinct from the C-terminal extension in bacterial TyrRSs, and is absent from yeast and lower animals (like *Caenorhabditis elegans*) (Liu et al., 2002) (Figure 1A). The C-domain itself also has cytokine activity. It is a structural and functional homolog to another cytokine known as endothelial monocyte activating polypeptide II (EMAPII) (Kleeman et al., 1997; Liu et al., 2002). Both EMAPII and the C-domain of TyrRS cause migration of mononuclear phagocytes (MPs) and PMNs, production of tumor necrosis factor-α and tissue factor by MPs, and release of myeloperoxidase from PMNs.

High resolution crystal structures of mini-TyrRS and of C-domain enabled reconstruction of the structure of the full-length enzyme which, in turn, provided the structural basis for cytokine activation (Yang et al., 2002, 2003a, 2004). This activation is postulated to be achieved by exposing a three amino acid motif—ELR—in the Rossmann-fold catalytic domain, after proteolytic removal of the C-domain. An ELR motif is critical for the pro-angiogenic activities of chemokines such as interleukin-8 (IL-8) (Baggiolini and Clark-Lewis, 1992). The importance of the ELR motif for cytokine activity of TyrRS was demonstrated by an experiment in which placement of ELR motif into (cytokine-inactive) yeast TyrRS led to gain of cytokine function (Liu et al., 2002). To support the hypothesis for cytokine activation, a rationally designed mutation (Y341A) to open up the conformation of TyrRS and expose the ELR motif without proteolytic cleavage was constructed. Significantly, Y341A TyrRS had the same cytokine activity as seen for mini-TyrRS (Yang et al., 2007a), strongly supporting the importance of the ELR motif for cytokine activity.

Because the aminoacylation activities of TyrRS and mini-TyrRS are the same, it is the core enzyme (mini-TyrRS) that provides a direct connection of aminoacylation and cell signaling. TyrRSs of lower eukaryotes lack the C-domain of the mammalian enzymes and are closely similar to the mini-TyrRS core enzyme, but appear not to have any cytokine activity. Thus, over evolution, the mammalian enzymes acquired the C-domain and adapted the mini-TyrRS core (by addition of ELR motif) for cytokine signaling that is not seen in the lower forms.

NIH-PA Author Manuscript

NIH-PA Author Manuscript

NIH-PA Author Manuscript

While yeast TyrRS gained cytokine activity when the ELR motif was transplanted (Liu et al., 2002), introduction of the ELR motif also stimulated aminoacylation activity, suggesting a potential correlation between the two activities. To understand how cytokine signaling could be introduced without loss of aminoacylation, we used our high-resolution structure to guide construction of variants that were investigated in a battery of assays. These variants were specifically designed to disrupt aminoacylation or cytokine signaling, and seeing whether there was "cross-talk" between these activities or whether they, in the context of the variants, were insulated from each other.

Results

Creating catalytic variants and investigating their cytokine function

Mini-TyrRS variant with disrupted catalytic activity—The aminoacylation reaction catalyzed by TyrRS occurs in two steps. In the first step, tyrosine is activated through condensation with ATP to generate Tyr-AMP (tyrosyl adenylate), with the release of pyrophosphate (PPi). In the second step, the activated amino acid (Tyr-AMP) is covalently appended to the 3′- end of $tRNA^{Tyr}$ to give Tyr-$tRNA^{Tyr}$ and AMP. These activities come from two distinct structurally segregated domains: a Rossmann-fold catalytic domain that is shared by all 10 class I tRNA synthetases and which houses the active site, and the anticodon recognition domain (Figure 1B). An 11 amino acid signature sequence peptide that ends in HIGH and a second peptide harboring KMSKS contribute to formation of the ATP binding site (Arnez et al., 1997; Webster et al., 1984). The signature peptides can have degenerated sequences. In human TyrRS, the second signature peptide has the specific sequence ^{222}KMSSS^{226}, where S224 and S226 play an important role in catalyzing formation of Tyr-AMP (Austin and First, 2002a). Thus, S224A or S226A reduced forward rate constant (for adenylate synthesis) by 7.5- and 60- fold, respectively, without significantly affecting substrate binding (Austin and First, 2002a).

We created S224A/S226A (KMSSS to KMASA) mini-TyrRS by site directed mutagenesis and tested its overall aminoacylation activity by monitoring the incorporation of tyrosine into $tRNA^{Tyr}$ to form Tyr-$tRNA^{Tyr}$. Compared to wild-type mini-TyrRS, mini-TyrRS(KMASA) has significantly reduced aminoacylation activity (Figure 2A). To confirm that the catalytic deficiency resulted from disruption of the first step of adenylate synthesis, as previously suggested (Austin and First, 2002a), we measured tyrosine-dependent ATP-PPi exchange, as an indication of synthesis of Tyr-AMP. As anticipated, mini-TyrRS(KMASA) was defective in this assay (Figure 2A, inset).

Aminoacylation defective mini-TyrRS variant retains cytokine activities—Next, the cytokine activities of mini-TyrRS(KMASA) were determined in two separate assays for cell signaling: Polymorphonuclear leukocyte (PMN) cell migration and angiogenesis in the chick chorioallantoic membrane assay. Mini-TyrRS stimulates migration of PMN cells purified from human blood (Wakasugi and Schimmel, 1999a). Using the same migration assay, we tested mini-TyrRS(KMASA), along with wild-type mini-TyrRS and IL-8 as positive controls, and untreated cells as a negative control. Both wild-type and mini-TyrRS(KMASA) had comparatively similar levels of stimulation of migration of PMNs. They also showed the expected dose-dependent bell shaped chemotaxis activity that had maximum migration at 10 nM (Figure 2B). This result suggested that the catalytically defective variant was fully active for cytokine signaling.

For further *in vivo* confirmation, we next carried out angiogenesis assays using chick chorioallantoic membranes (CAMs) to establish whether mini-TyrRS(KMASA) retained its pro-angiogenic activity. In this *in vivo* model, angiogenic factors stimulate new vessels to grow vertically from the surface of the CAM membrane into a collagen and nylon mesh implant. As

NIH-PA Author Manuscript

NIH-PA Author Manuscript

NIH-PA Author Manuscript

a positive control, a well-established cytokine, the potent angiogenic vascular endothelial growth factor (VEGF), was used to stimulate angiogenesis, while phosphate-buffered saline was used as a negative control. When compared to buffer alone, both mini-TyrRS and mini-TyrRS(KMASA) stimulated new vessel growth into the collagen matrix (Figure 2C).

Thus, according to both PMN cell migration and CAM angiogenesis, disruption of aminoacylation, at the ATP binding site, does not affect two cell signaling functions of mini-TyrRS.

Mini-TyrRS variants with disrupted tyrosine binding capacity—We next examined if the tyrosine binding capability of mini-TyrRS contributed in any way to its cytokine activity. Based on the crystal structure of mini-TyrRS, Tyr39 and Asp173 are required for tyrosine binding (Yang et al., 2003b). Tyr39 is conserved in eukaryotic, archaeal, and one of the two groups of bacterial TyrRSs, while Asp173 is ubiquitously conserved through evolution. A Y43G substitution in yeast TyrRS (corresponds to Y39G in the human enzyme) increased the K_m for tyrosine from 0.014 mM to 1.19 mM (Ohno et al., 2001). In order to study the effect of abrogation of tyrosine binding capacity on the cytokine function of TyrRS, we adopted a similar rational mutagenesis approach in which we constructed single amino acid variants—Y39A, D173A--and the combined Y39A/D173A two amino acid variant. Recombinant wild-type mini-TyrRS and its variants were purified from *E. coli*. Comparison of wild-type with its variants using circular dichroism spectroscopy indicated that the proteins had similar secondary structures (Figure S1A) Importantly, all three variants had significantly reduced aminoacylation activity (Figure 3A).

To confirm that the variants were defective in tyrosine binding, we used an equilibrium dialysis binding assay to determine the dissociation constants for tyrosine binding to wild-type mini-TyrRS and its variants. In this assay mini-TyrRS or its variants were incubated with different concentrations of [^{3}H]Tyr across a semipermeable membrane. After the samples reached equilibrium, the amount of free tyrosine and tyrosine bound to the protein was determined and used to calculate the dissociation constant (K_d), as explained in Experimental Procedures. The K_d for mini-TyrRS was 30 μM (Figure S2A). The Y39A/D173A variant had greater than 25-fold reduction in tyrosine binding with a K_d of more than 700 μM (Figure S2B). This result showed that, indeed, the Y39A/D173A mini-TyrRS has severely lost its tyrosine binding capacity.

Tyrosine binding pocket mini-TyrRS variants retain cytokine activity—Cytokine activities of the tyrosine-binding-pocket variants of mini-TyrRS were studied by PMN cell and endothelial cell migration assays. As described above, PMNs were freshly isolated from human blood. In these assays, IL-8 was used as a positive control and a mini-TyrRS(ELQ) variant (Arg93 to Gln) that lacks cytokine activity (Wakasugi and Schimmel, 1999a) was used as a negative control. The two single amino acid variants (Y39A and D173A), and the double amino acid variant (Y39A/D173A), caused migration of cells similar to that observed for mini-TyrRS (Figure 3B). Although the activity was slightly less than mini-TyrRS, it followed the bell shaped curve typical of such cytokines, consistent with mini-TyrRS variants binding to their cognate cell surface receptor and triggering downstream signaling events.

We next tested the activity of variants in an endothelial cell migration assay. In these experiments, wounds of defined characteristics were created in monolayers of human umbilical vein endothelial cells (HUVECs). Mini-TyrRS or the tyrosine-binding-pocket variants were added to the media to test for their ability to close the wound by stimulating cell migration. Wound monolayers closed in response to vascular endothelial growth factor (VEGF) within 6 hr (used as a positive control) (Figure 3C). In cells treated with mini-TyrRS or its variants, a similar migration of cells into the wounded monolayer was seen.

NIH-PA Author Manuscript

NIH-PA Author Manuscript

NIH-PA Author Manuscript

Taken together, the results of PMN and endothelial cell migration assays demonstrated that amino acid changes in the tyrosine binding pocket do not impact the cytokine activities of mini-TyrRS. We further investigated the insulation of the tyrosine binding pocket from cytokine function by performing the PMN migration assay with mini-TyrRS under the influence of Tyr-SA (5′-O-[N-L-tyrosyl)sulfamoyl]adenosine, an analogue of Tyr-AMP) that is a potent inhibitor of aminoacylation and binding of tyrosine. Tyr-SA did not inhibit the cytokine activity of mini-TyrRS (Figure S3).

Cytokine-disruption variants of the ELR motif on a surface helix and effect on aminoacylation

Mini-TyrRS variants with disrupted cytokine function—A surface helix (α5) on mini-TyrRS encodes an ELR motif (Figure 1B) that functions like the ELR tripeptide in CXC cytokines like IL-8. Having established that the cytokine activity of mini-TyrRS is not affected by the aminoacylation activity *per se*, we next addressed the converse—do mutations that interfere with cytokine activity also affect aminoacylation? Previously, we demonstrated that substitution of Arg93 within the ELR motif (to create mini-TyrRS(ELQ)) abolished the PMN cell migration activity and the binding to PMN cells (Wakasugi and Schimmel, 1999a). Further the ELQ variant did not induce endothelial cell (HUVEC) migration *in vitro* and angiogenesis *in vivo* (Wakasugi et al., 2002b).

To further dissect the ELR motif and the relationship, if any, between the cytokine and aminoacylation activities, we changed the first and the second residues of the ELR motif to their corresponding residues in the cytokine-inactive yeast TyrRS, namely, E91 to N (mini-TyrRS(NLR)) and L92 to Y (mini-TyrRS(EYR)). In addition, we included the previously created R93 to Q variant (mini-TyrRS(ELQ)) in the analyses. All variants were purified by recombinant expression in *E. coli* and, based on circular dichroism analysis, had secondary structure similar to that of mini-TyrRS (Figure S1B).

The effect of replacing each of the ELR residues on the cytokine activity of mini-TyrRS was evaluated by the PMN migration and the endothelial cell wound healing assays. The effect of these single amino acid changes on the PMN cell migration activity of mini-TyrRS is shown in Figure 4A. As described above, mini-TyrRS induced migration of PMN cells in a concentration-dependent manner. However, mini-TyrRS(NLR) and mini-TyrRS(ELQ) were inactive while mini-TyrRS(EYR) showed only a minimal activity in the PMN cell migration assay. Thus, each of the three ELR residues is important for cytokine function. As expected, full-length TyrRS had no influence on migration.

To further test if position 92 would tolerate any change, we also created and tested another variant L92 to E (mini-TyrRS(EER)), based on the residue at the corresponding position in the TyrRS sequence of the mosquito, *Anopheles gambiae*. Again, mini-TyrRS(EER) did not cause migration of PMN cells (Figure S4), confirming the specificity and importance of L92 residue for the cytokine activity.

Figure 4B shows the results of an endothelial cell wound healing assay. As described above, in mini-TyrRS treated samples, closure of the wounded monolayer was observed. In contrast to mini-TyrRS, all of the three single amino acid ELR variants did not cause migration of endothelial cells. Although, migration caused by mini-TyrRS(EYR) was slightly higher as compared to the other two ELR variants, the activity itself was not statistically significant as compared to the control. Mini-TyrRS(EYR) was also inactive for angiogenesis in the ischemic mouse ear (Cheng et al., 2008). Overall, the three residues of the ELR motif are important for mini-TyrRS cytokine activity. Similar result earlier demonstrated the importance of mini-TyrRS ELR motif during transactivation of VEGFR2 and endothelial cell tube formation (Greenberg et al., 2008). As expected, full-length TyrRS did not induce migration of cells.

NIH-PA Author Manuscript

NIH-PA Author Manuscript

NIH-PA Author Manuscript

Thus, these migration assays clearly demonstrated the requirement of having an intact ELR motif for the cytokine activity of mini-TyrRS.

Mini-TyrRS ELR variants retain catalytic activity—The next experiments determined how amino acid changes in the ELR motif—critical for cytokine activity—affect aminoacylation. From the crystal structure of mini-TyrRS, the ELR motif is located on a long α-helix (α5) on the surface of the Rossmann-fold catalytic domain (Figure 1B) (Yang et al., 2002). The three residues of the ELR motif form almost a full helical turn with the first two residues E and L being solvent-exposed and available for interactions with the cognate cellular receptor.

Replacement of E and L of the ELR motif abolished cytokine activity, but had little effect on aminoacylation activity. Mini-TyrRS(EYR) has wild-type-like aminoacylation activity. Mini-TyrRS(NLR) has a small decrease in aminoacylation activity (Figure 4C), possibly due to loss of H-bonding interactions of E91 with surrounding residues that may have a slight effect of stabilizing the active site. Nevertheless, the decrease in activity is small, especially when the change in free energy is considered. Thus, at the phenotypic level, these amino acid changes clearly separate aminoacylation and cytokine activities, in the exact reverse as was shown with the changes in the active site for aminoacylation that did not perturb cytokine function.

R93-dependent positioning of the ELR-containing helix supports simultaneous retention of cytokine and aminoacylation activities—We figured that replacement of R93 was more likely to affect aminoacylation as compared to the first two residues (EL), because R93 structurally bridges the parts for aminoacylation with the ELR motif (Yang et al., 2002). Particularly, R93 is in the center of a H-bonding network that stabilizes the conformation of the active site through interaction with the peptide harboring the “HIGH” signature sequence (Figure 1B, inset). Thus, we speculated that replacement of R93 would most likely disturb catalytic in addition to cytokine activity. This speculation was confirmed with experiments that showed that mini-TyrRS(ELQ) had significantly reduced aminoacylation activity, consistent with a perturbation of the H-bonding network that provides conformational stability near the active site (Figure 4C). A follow-up ATP-PPi exchange assay was performed on the ELQ variant to confirm that the synthesis of Tyr-AMP was affected. Indeed, mini-TyrRS(ELQ) had significantly reduced activity in this assay, showing that this variant was defective for synthesis of Tyr-AMP (Figure 4C, inset). Thus, R93 links the expanded cytokine function with aminoacylation, and its substitution disrupts both activities of mini-TyrRS.

Discusssion

Little is known of how novel functions of tRNA synthetases were developed in the context of their aminoacylation function. Simple domain fusions that bring in new functions appear to be a straightforward way to bring in new activities without disturbing aminoacylation. For example, in the case of the EMAPII-like C-domain of TyrRS, two proteins (mini-TyrRS and C-domain) were simply fused together in a way that did not disturb the essential aminoacylation function of the mini-TyrRS part of TyrRS. A similar situation occurs with the unusual glutamyl-prolyl fusion synthetase, where the linker between the two synthetases provides the determinants for regulation of translation of mRNAs related to the inflammatory response (Jia et al., 2008; Ray and Fox, 2007; Sampath et al., 2004). Thus, these examples show that one strategy for a synthetase to gain an expanded function is by acquisition of a new domain.

However, the potent cytokine activity of mini-TyrRS does not come from a separate, fused domain. The activity arises from within the core catalytic unit itself. In this instance, a long helix that is part of the Rossmann-fold of all class I tRNA synthetases was exploited (Figure 1B). This helix is located on the surface, and not involved with forming a part of the active

NIH-PA Author Manuscript

NIH-PA Author Manuscript

NIH-PA Author Manuscript

site. By having a surface location, it is in principle accessible for interactions with a cellular receptor and, through evolution, could be exploited by introducing sequence changes that facilitate receptor binding.

In this connection, earlier work suggested that selective pressure to gain and retain an expanded function in a tRNA synthetase would be strongest when a mutation that disrupted the newly developing function also disrupted the essential aminoacylation activity (Yang et al., 2007b). While substitutions of either the E or L of the ELR motif (in the surface helix) of human TyrRS ablated cytokine activities without having a major effect on aminoacylation, the R93Q substitution ablated both cytokine and aminoacylation functions. Significantly, of the three amino acids—ELR—only R93 is conserved for almost all eukaryotes. This conservation may have been critical for the selective pressure that enabled development of the cytokine function. Therefore, while “R” was present in lower eukaryotes, the E and L combination only emerged in higher eukaryotes like mammals.

Thus, our results suggest that the development of the cytokine function of TyrRS exploited two residues of a surface helix that could be varied (positions 91 and 92 of the ELR tripeptide) without disruption of aminoacylation. At the same time, an adjacent residue (R93) linked the developing cytokine activity to the essential aminoacylation function. In addition to forcing retention of R93, this strategy probably limited the possibilities for variations at positions 91 and 92, with only those that did not alter the conformation of R93, and its role to stabilize the active site.

An ELR motif preceding the first cysteine at the N-terminus is a hallmark for CXC-chemokines that are angiogenic, such as IL-8. Each residue of the ELR motif in CXC-chemokines is critical for receptor binding and neutrophil activation (Hebert et al., 1991). Here we showed that each of the same three residues is also essential for the cytokine functions of mini-TyrRS. It is this ELR motif that is believed to be essential for the ability of mini-TyrRS to compete with IL-8 for the CXCR1 receptor (Wakasugi and Schimmel, 1999a). Interestingly, the ELR motif of mini-TyrRS is encoded by a surface helix, but this motif in IL-8 is located in a flexible region (Baldwin et al., 1991). Thus, we speculate that the flexible N-terminal sequence of the ELR-containing CXC-chemokines adopts a helical conformation upon receptor binding (Figure 5).

Dominant mutations in human TyrRS are amongst the genetic causes of Charcot-Marie-Tooth (CMT) disease (Jordanova et al., 2006). While the cytokine activities of the proteins encoded by the known mutant alleles have not been investigated, work is underway to understand the link between cytokine activity and the CMT-disease phenotype. Regardless of the outcome, the present investigation establishes the idea that new motifs conferring novel activities can be added to even a highly conserved part of the historical tRNA synthetase architecture, with little effect on aminoacylation. Because of this functional separation, potential disease-associated mutations can affect only the cytokine function, but not the essential aminoacylation function and therefore, in principle, can be carried forward in the population.

Significance

Heritable mutations in tRNA synthetases are causally linked to disease. While aminoacyl-tRNA synthetases are universal proteins known for catalysis of aminoacylation, the later-developed expanded functions of many mammalian synthetases in cytokine signaling and regulatory pathways are considered to be the main connection with diseases. This work shows that the ancient conserved architecture of tRNA synthetases can protect the essential aminoacylation function, when new cell-signaling epitopes are introduced near the catalytic site. Consequently, because of the protective isolation of the active site, disease-causing mutations that affect only cell signaling can arise and be transmitted.

NIH-PA Author Manuscript

NIH-PA Author Manuscript

NIH-PA Author Manuscript

Experimental Procedures

Plasmids

Mutant human mini-TyrRS constructs were generated using QuikChange site-directed mutagenesis kit (Stratagene, La Jolla, CA) and using a plasmid encoding the gene for wild-type human mini-TyrRS (Wakasugi and Schimmel, 1999a) as the template for PCR mutagenesis reactions. Synthetic oligonucleotides were purchased from Invitrogen Corporation (Carlsbad, CA). All proteins were expressed with a C-terminal His-tag to facilitate purification.

Protein purification and removal of endotoxin

Wild-type human mini-TyrRS and its variants were purified as described previously (Wakasugi and Schimmel, 1999a). Recombinant proteins were overexpressed in *Escherichia coli* strain BL21-CodonPlus (DE3)-RIL (Stratagene, La Jolla, CA). Cultures were grown in Luria Broth until log phase and then were induced with 1 mM isopropyl β-D-thiogalactopyranoside (IPTG) (Novagen, Madison, WI) for 4 hr. Cells were harvested by centrifugation, lysed on ice by sonication in column buffer (20 mM Tris-HCl (pH 7.9), 500 mM sodium chloride, 30 mM imidazole and 5 mM β-mercaptoethanol), and the lysate cleared by centrifugation at 35,000g for 30 min. The supernatant was loaded onto a Ni-NTA affinity column (Qiagen, Valencia, CA) pre-equilibrated with column buffer. The column was washed with column buffer containing 0.1% triton-X 114 (Sigma, St. Louis, MO) to dissociate lipopolysaccharide (endotoxin) from the protein, followed by additional column buffer to remove residual detergent. The protein was eluted with a gradient of 30-250 mM imidazole in column buffer and stored in phosphate buffered saline (PBS) (pH 7.4)/50% glycerol, 2 mM dithiothreitol and 1 μM zinc sulphate. All purified proteins were more than 95% pure as judged by polyacrylamide gel electrophoresis (4–12% Bis-Tris NuPAGE gels, Invitrogen, Carlsbad, CA). Protein concentration was determined using the Bio-Rad Protein Assay reagent (Bio-Rad, Hercules, CA) with bovine serum albumin (Sigma, St. Louis, MO) as a standard. Endotoxin was removed using an EndoTrap Red column (Lonza, Basel, Switzerland) from samples used for angiogenesis assays and endotoxin concentrations determined using Kinetic-QCL Limulus Amebocyte Lysate (LAL) assay (Lonza).

Amino acid activation assay

Amino acid activation was assessed by monitoring the tyrosine-dependent ATP-pyrophosphate (PPi) exchange reaction (Calendar and Berg, 1966) at 37 °C. Each reaction mixture contained 100 mM Tris-HCl (pH 7.8), 5 mM β-mercaptoethanol, 2 mM magnesium chloride, 1 mM ATP, 2 mM sodium pyrophosphate or sodium [^{32}P] pyrophosphate (Perkin Elmer, specific activity: 37 TBq/mmol), 100 μg/ml bovine serum albumin, 2 mM tyrosine, and wild-type mini-TyrRS or its variants. Aliquots were removed at various time points and quenched into 200 mM sodium pyrophosphate, 11% perchloric acid, and 4% (w/v) activated charcoal. The reaction mixture was filtered through a 0.45 μm centrifugal filter (Fisher, Pittsburg, PA) and the charcoal was washed twice with a solution containing 200 mM sodium pyrophosphate and 1% perchloric acid. Charcoal-absorbed [^{32}P]ATP was quantified by scintillation counting.

Aminoacylation assay

Aminoacylation activity was determined at ambient temperature in 150 mM Tris-HCl (pH 7.5), 150 mM potassium chloride, 10 mM magnesium chloride, 10 mM β-mercaptoethanol, 4 mM ATP, and 10 μM tyrosine (including 3 μM [^{3}H]-tyrosine (GE Healthcare, Specific activity: 3.7 TBq/mmol)). Human tRNA^{Tyr} was prepared as described earlier (Liu et al., 2002). Before each assay, 100 μM human tRNA^{Tyr} was annealed by heating at 65 °C for five minutes and cooled to room temperature. Reactions were initiated by the addition of enzyme (10 nM) to the reaction

NIH-PA Author Manuscript

NIH-PA Author Manuscript

NIH-PA Author Manuscript

mixture. Aliquots were taken at fixed intervals and spotted onto Whatman filter discs saturated with 5% trichloroacetic acid and dried. The filters were placed into ice-cold 5% trichloroacetic acid, washed three times with fresh 5% trichloroacetic acid at 4 °C and once with 95% ethanol. The level of aminoacylation of tRNA was quantitated by liquid scintillation counting.

Equilibrium binding studies

Equilibrium dialysis was performed using a modification of the method described earlier (Austin and First, 2002b). Prior to the binding experiment, protein stocks were dialyzed in PBS (pH 7.4). The experiment was performed by placing protein (20–40 μM) and tyrosine (3.6–1000 μM, [^{3}H]-labeled (GE Heathcare, Specific activity: 3.7 TBq/mmol)) suspended in PBS in the two chambers on either side of a semipermeable membrane. After overnight dialysis at 20 °C, the radioactivity in both the chambers was measured by scintillation counting and free and bound tyrosine calculated at each concentration. Dissociation constants were obtained by nonlinear and linear curve fitting using equation 1 and 2, respectively (Scatchard, 1949).

$$[\mathrm{Tyr}]_{\mathrm{bound}}/[\mathrm{E}]_{\mathrm{T}}=\mathrm{n}[\mathrm{Tyr}]_{\mathrm{free}}/\left([\mathrm{Tyr}]_{\mathrm{free}}+\mathrm{K}_{\mathrm{Tyr}}\right) \qquad \text{Equation (1)}$$

$$[\mathrm{Tyr}]_{\mathrm{bound}}/[\mathrm{Tyr}]_{\mathrm{free}}=\left(-1/\mathrm{K}_{\mathrm{Tyr}}\right)[\mathrm{Tyr}]_{\mathrm{bound}}+\left(\mathrm{n}[\mathrm{E}]_{\mathrm{T}}/\mathrm{K}_{\mathrm{Tyr}}\right) \qquad \text{Equation (2)}$$

where, K_{Tyr} is the dissociation constant for tyrosine, $[Tyr]_{bound}$ is the concentration of tyrosine bound to the enzyme, $[Tyr]_{free}$ is the concentration of unbound tyrosine at equilibrium, n is the number of binding sites, and $[E]_T$ is the total enzyme concentration.

Polymorphonuclear Leukocyte (PMN) Migration Assay

Human PMNs were prepared from heparin treated whole blood from normal healthy volunteers as described (Liu et al., 2002). Human PMNs were isolated from blood by centrifugation (700g) over Histopaque 1077 and 1119 as described by the manufacturer (Sigma, St. Louis, MO), washed three times with PBS, and suspended in RPMI 1640 (ATCC, Manassas, VA) containing heat inactivated fetal bovine serum (FBS) (0.5%, Invitrogen) at a concentration of 4.0×10^5 cells/ml.

Cell migration was performed in a micro-chemotaxis chamber ChemoTX (NeuroProbe, Gaithersburg, MD) as described (Liu et al., 2002). Proteins, diluted in RPMI 1640, were placed in the lower wells of the chamber separated by a polycarbonate filter (5 μm pore) without polyvinylpyrrolidone (Neuro Probe) from 50 μl of the PMN cell suspension in the upper chamber. Cells were allowed to migrate for 30 min at 37 °C in a 5% CO_2 incubator. After incubation, the membrane was removed from the chemotaxis chamber and the non-migrating cells carefully washed from the upper side of the membrane. The membrane was stained with a Diff-Quik stain set (VWR International, West Chester, PA) and the cells migrated to the lower side of the membrane were counted under a light microscope. Samples were run in triplicate and cells counted in five high power fields (HPFs) for each sample.

Endothelial Cell Migration assay

Endothelial cell migration assays were performed as described earlier with some modifications (Yang et al., 2007a). Human umbilical vein endothelial cells (HUVECs) (Lonza) were maintained in endothelial growth media (EGM) (Lonza) supplemented with 10% FBS in an atmosphere of 5% CO_2 in air at 37 °C according to the supplier's instructions. For the migration assay, HUVECs were plated at a density of 3×10^5 cells/well of a 6-well plate in EGM

NIH-PA Author Manuscript

NIH-PA Author Manuscript

NIH-PA Author Manuscript

containing 10% FBS and grown to confluent monolayers. Cells were starved in media containing no FBS for 16 hr and wounded across the well with a pipette tip. The wounded layers were washed twice with serum free media to remove cell debris and cells allowed to migrate with and without different mini-TyrRS proteins and control factors. Images of the cell-free wound area were taken at 0 and 6 hr and analyzed using image analysis software (NIH ImageJ 1.33). The wound healing effect was calculated as the percentage of the remaining cell-free area compared with the area of the initial wound and used to obtain the percentage area closed for each condition.

Chick chorioallantoic membrane (CAM) angiogenesis assay

Chicken embryo cultures were prepared as described by Seandel and colleagues (Seandel et al., 2001). Fertilized COFAL-negative eggs (SPAFAS, North Franklin, CT) were incubated horizontally at 37 °C with 60% humidity in a manual egg turning incubator (Lyon Electric Company, Inc. Chula Vista, CA). After 3.5 days, the shells were scored equatorially with a rotary wheel (Dremel, Racine, WI) and manually opened to transfer embryos into sterile plastic weigh boats (medium, 9 × 9 × 2.5 cm, VWR, San Diego, CA). The weigh boats were covered with square 100 × 100 mm petri dishes (no. 4021, Nunc, Rochester, NY) and embryos were maintained in a cell culture incubator (NAPCO, Winchester, VA) at 37 °C with 90% humidity.

Angiogenic effects of mini-TyrRS and its variants were tested on CAMs as described earlier (Seandel et al., 2001). Briefly, 8 parts of pure type I collagen (3.1 mg/ml) (Cohesion, Palo Alto, CA) was neutralized with 1 part 10X PBS and 1 part 0.1 N sodium hydroxide. To maintain pH 7.4, HEPES (pH 7.4) was added to a final concentration of 20 mM. Two parts neutralized collagen solution was combined with sterile PBS-containing bovine serum albumin (final concentration 1 mg/ml), with or without VEGF (PeproTech, Rocky Hill, NJ), mini-TyrRS, or mini-TyrRS variants. The final concentration of all protein samples was 1 μM. Collagen/protein solution (30 μl) was placed atop two layers of sterile nylon mesh (Nitex, lower layer, 4 × 4 mm; upper layer, 2 × 2 mm) (Sefar American Inc, Kansas City, MO). These collagen/mesh implants were incubated at 37 °C with 90% humidity for 1.5–2 hr to polymerize the collagen matrix. After polymerization, the implants were placed on the CAM of a 10-day old chick embryo using sterile forceps. Four implants were placed on each CAM, with at least one negative control (PBS) and one positive control (VEGF) per embryo. The embryos were returned to the incubator and observed on day 13 with a stereomicroscope (Dolan-Jenner Industries, Lawrence, MA). Distinct blood vessels appearing in the collagen matrix at or above the plane of the top mesh were identified. Each square in the top mesh grid was scored for the presence or absence of vessels to give a proportion of positive boxes/total boxes counted.

Supplementary Material

Refer to Web version on PubMed Central for supplementary material.

Acknowledgments

This work was supported by grants CA 92577 and GM 15539 from the National Institutes of Health and by a fellowship from the National Foundation for Cancer Research. We thank Prof. Paul Schimmel for constructive ideas, discussions and support during this work and critical reading and editing of the manuscript. We thank Dr. Andres Zijlstra and Dr. James P. Quigley for assistance with the chick CAM assays.

References

Antonellis A, Green ED. The role of aminoacyl-tRNA synthetases in genetic diseases. Annu Rev Genomics Hum Genet 2008;9:87–107. [PubMed: 18767960]

Antonellis A, Lee-Lin SQ, Wasterlain A, Leo P, Quezado M, Goldfarb LG, Myung K, Burgess S, Fischbeck KH, Green ED. Functional analyses of glycyl-tRNA synthetase mutations suggest a key

NIH-PA Author Manuscript

NIH-PA Author Manuscript

NIH-PA Author Manuscript

role for tRNA-charging enzymes in peripheral axons. J Neurosci 2006;26:10397–10406. [PubMed: 17035524]

Arnez JG, Moras D. Structural and functional considerations of the aminoacylation reaction. Trends Biochem Sci 1997;22:211–216. [PubMed: 9204708]

Austin J, First EA. Comparison of the catalytic roles played by the KMSKS motif in the human and *Bacillus stearothermophilus* tyrosyl-tRNA synthetases. J Biol Chem 2002a;277:28394–28399. [PubMed: 12016229]

Austin J, First EA. Catalysis of tyrosyl-adenylate formation by the human tyrosyl-tRNA synthetase. J Biol Chem 2002b;277:14812–14820. [PubMed: 11856731]

Baggiolini M, Clark-Lewis I. Interleukin-8, a chemotactic and inflammatory cytokine. FEBS Lett 1992;307:97–101. [PubMed: 1639201]

Baldwin ET, Weber IT, St Charles R, Xuan JC, Appella E, Yamada M, Matsushima K, Edwards BF, Clore GM, Gronenborn AM, Wlodawer A. Crystal structure of interleukin-8: Symbiosis of NMR and crystallography. Proc Natl Acad Sci USA 1991;88:502–506. [PubMed: 1988949]

Calendar R, Berg P. The catalytic properties of tyrosyl ribonucleic acid synthases from *Escherichia coli* and *Bacillus subtilis*. Biochemistry 1966;5:1690–1695. [PubMed: 4289778]

Cheng G, Zhang H, Yang X, Tzima E, Ewalt KL, Schimmel P, Faber JE. Effect of mini-tyrosyl-tRNA synthetase on ischemic angiogenesis, leukocyte recruitment and vascular permeability. Am J Physiol Regul Integr Comp Physiol 2008;295:R1138–1146. [PubMed: 18753262]

DeLano, WL. DeLano Scientific; Palo Alto, CA, USA: 2002. The PyMOL Molecular Graphics System. http://www.pymol.org

Greenberg Y, King M, Kiosses WB, Ewalt K, Yang X, Schimmel P, Reader JS, Tzima E. The novel fragment of tyrosyl tRNA synthetase, mini-TyrRS, is secreted to induce an angiogenic response in endothelial cells. FASEB J 2008;22:1597–1605. [PubMed: 18165356]

Hebert CA, Vitangcol RV, Baker JB. Scanning mutagenesis of interleukin-8 identifies a cluster of residues required for receptor binding. J Biol Chem 1991;266:18989–18994. [PubMed: 1918013]

Howard OM, Dong HF, Yang D, Raben N, Nagaraju K, Rosen A, Casciola-Rosen L, Hartlein M, Kron M, Yiadom K, Dwivedi S, Plotz PH, Oppenheim JJ. Histidyl-tRNA synthetase and asparaginyl-tRNA synthetase, autoantigens in myositis, activate chemokine receptors on T lymphocytes and immature dendritic cells. J Exp Med 2002;196:781–791. [PubMed: 12235211]

Javanbakht H, Halwani R, Cen S, Saadatmand J, Musier-Forsyth K, Gottlinger H, Kleiman L. The interaction between HIV-1 Gag and human lysyl-tRNA synthetase during viral assembly. J Biol Chem 2003;278:27644–27651. [PubMed: 12756246]

Jia J, Arif A, Ray PS, Fox PL. WHEP domains direct noncanonical function of glutamyl-prolyl tRNA synthetase in translational control of gene expression. Mol Cell 2008;29:679–690. [PubMed: 18374644]

Jordanova A, Irobi J, Thomas FP, Van Dijck P, Meerschaert K, Dewil M, Dierick I, Jacobs A, De Vriendt E, Guergueltcheva V, Rao CV, Tournev I, Gondim FA, D'Hooghe M, Van Gerwen V, Callaerts P, Van Den Bosch L, Timmermans JP, Robberecht W, Gettemans J, Thevelein JM, De Jonghe P, Kremensky I, Timmerman V. Disrupted function and axonal distribution of mutant tyrosyl-tRNA synthetase in dominant intermediate Charcot-Marie-Tooth neuropathy. Nat Genet 2006;38:197–202. [PubMed: 16429158]

Kleeman TA, Wei D, Simpson KL, First EA. Human tyrosyl-tRNA synthetase shares amino acid sequence homology with a putative cytokine. J Biol Chem 1997;272:14420–14425. [PubMed: 9162081]

Ko YG, Kim EY, Kim T, Park H, Park HS, Choi EJ, Kim S. Glutamine-dependent antiapoptotic interaction of human glutaminyl-tRNA synthetase with apoptosis signal-regulating kinase 1. J Biol Chem 2001;276:6030–6036. [PubMed: 11096076]

Lee SW, Cho BH, Park SG, Kim S. Aminoacyl-tRNA synthetase complexes: beyond translation. J Cell Sci 2004;117:3725–3734. [PubMed: 15286174]

Liu J, Yang XL, Ewalt KL, Schimmel P. Mutational switching of a yeast tRNA synthetase into a mammalian-like synthetase cytokine. Biochemistry 2002;41:14232–14237. [PubMed: 12450387]

NIH-PA Author Manuscript

NIH-PA Author Manuscript

NIH-PA Author Manuscript

Martinis SA, Plateau P, Cavarelli J, Florentz C. Aminoacyl-tRNA synthetases: a family of expanding functions. Mittelwihr, France, October 10-15, 1999. EMBO J 1999;18:4591–4596. [PubMed: 10469639]

Nangle LA, Zhang W, Xie W, Yang XL, Schimmel P. Charcot-Marie-Tooth disease-associated mutant tRNA synthetases linked to altered dimer interface and neurite distribution defect. Proc Natl Acad Sci USA 2007;104:11239–11244. [PubMed: 17595294]

Ohno S, Yokogawa T, Nishikawa K. Changing the amino acid specificity of yeast tyrosyl-tRNA synthetase by genetic engineering. J Biochem 2001;130:417–423. [PubMed: 11530018]

Park SG, Ewalt KL, Kim S. Functional expansion of aminoacyl-tRNA synthetases and their interacting factors: new perspectives on housekeepers. Trends Biochem Sci 2005;30:569–574. [PubMed: 16125937]

Park SG, Schimmel P, Kim S. Aminoacyl tRNA synthetases and their connections to disease. Proc Natl Acad Sci USA 2008;105:11043–11049. [PubMed: 18682559]

Ray PS, Fox PL. A post-transcriptional pathway represses monocyte VEGF-A expression and angiogenic activity. EMBO J 2007;26:3360–3372. [PubMed: 17611605]

Sampath P, Mazumder B, Seshadri V, Gerber CA, Chavatte L, Kinter M, Ting SM, Dignam JD, Kim S, Driscoll DM, Fox PL. Noncanonical function of glutamyl-prolyl-tRNA synthetase: gene-specific silencing of translation. Cell 2004;119:195–208. [PubMed: 15479637]

Scatchard G. The attractions of proteins for small molecules and ions. Ann N Y Acad Sci 1949;51:660–672.

Scheper GC, van der Klok T, van Andel RJ, van Berkel CG, Sissler M, Smet J, Muravina TI, Serkov SV, Uziel G, Bugiani M, Schiffmann R, Krageloh-Mann I, Smeitink JA, Florentz C, Van Coster R, Pronk JC, van der Knaap MS. Mitochondrial aspartyl-tRNA synthetase deficiency causes leukoencephalopathy with brain stem and spinal cord involvement and lactate elevation. Nat Genet 2007;39:534–539. [PubMed: 17384640]

Seandel M, Noack-Kunnmann K, Zhu D, Aimes RT, Quigley JP. Growth factor-induced angiogenesis in vivo requires specific cleavage of fibrillar type I collagen. Blood 2001;97:2323–2332. [PubMed: 11290594]

Seburn KL, Nangle LA, Cox GA, Schimmel P, Burgess RW. An active dominant mutation of glycyl-tRNA synthetase causes neuropathy in a Charcot-Marie-Tooth 2D mouse model. Neuron 2006;51:715–726. [PubMed: 16982418]

Wakasugi K, Schimmel P. Two distinct cytokines released from a human aminoacyl-tRNA synthetase. Science 1999a;284:147–151. [PubMed: 10102815]

Wakasugi K, Schimmel P. Highly differentiated motifs responsible for two cytokine activities of a split human tRNA synthetase. J Biol Chem 1999b;274:23155–23159. [PubMed: 10438485]

Wakasugi K, Slike BM, Hood J, Ewalt KL, Cheresh DA, Schimmel P. Induction of angiogenesis by a fragment of human tyrosyl-tRNA synthetase. J Biol Chem 2002a;277:20124–20126. [PubMed: 11956181]

Wakasugi K, Slike BM, Hood J, Otani A, Ewalt KL, Friedlander M, Cheresh DA, Schimmel P. A human aminoacyl-tRNA synthetase as a regulator of angiogenesis. Proc Natl Acad Sci USA 2002b;99:173–177. [PubMed: 11773626]

Webster T, Tsai H, Kula M, Mackie GA, Schimmel P. Specific sequence homology and three-dimensional structure of an aminoacyl transfer RNA synthetase. Science 1984;226:1315–1317. [PubMed: 6390679]

Yang XL, Skene RJ, McRee DE, Schimmel P. Crystal structure of a human aminoacyl-tRNA synthetase cytokine. Proc Natl Acad Sci USA 2002;99:15369–15374. [PubMed: 12427973]

Yang XL, Liu J, Skene RJ, McRee DE, Schimmel P. Crystal structure of an EMAP-II like cytokine released from a human tRNA synthetase. Helvetica 2003a;86:1246–1257.

Yang XL, Otero FJ, Skene RJ, McRee DE, Schimmel P, Ribas de Pouplana L. Crystal structures that suggest late development of genetic code components for differentiating aromatic side chains. Proc Natl Acad Sci USA 2003b;100:15376–15380. [PubMed: 14671330]

Yang XL, Schimmel P, Ewalt KL. Relationship of two human tRNA synthetases used in cell signaling. Trends Biochem Sci 2004;29:250–256. [PubMed: 15130561]

NIH-PA Author Manuscript

NIH-PA Author Manuscript

NIH-PA Author Manuscript

Yang XL, Kapoor M, Otero FJ, Slike BM, Tsuruta H, Frausto R, Bates A, Ewalt KL, Cheresh DA, Schimmel P. Gain-of-function mutational activation of human tRNA synthetase procytokine. Chem Biol 2007a;14:1323–1333. [PubMed: 18096501]

Yang XL, Guo M, Kapoor M, Ewalt KL, Otero FJ, Skene RJ, McRee DE, Schimmel P. Functional and crystal structure analysis of active site adaptations of a potent anti-angiogenic human tRNA synthetase. Structure 2007b;15:793–805. [PubMed: 17637340]

NIH-PA Author Manuscript

NIH-PA Author Manuscript

NIH-PA Author Manuscript

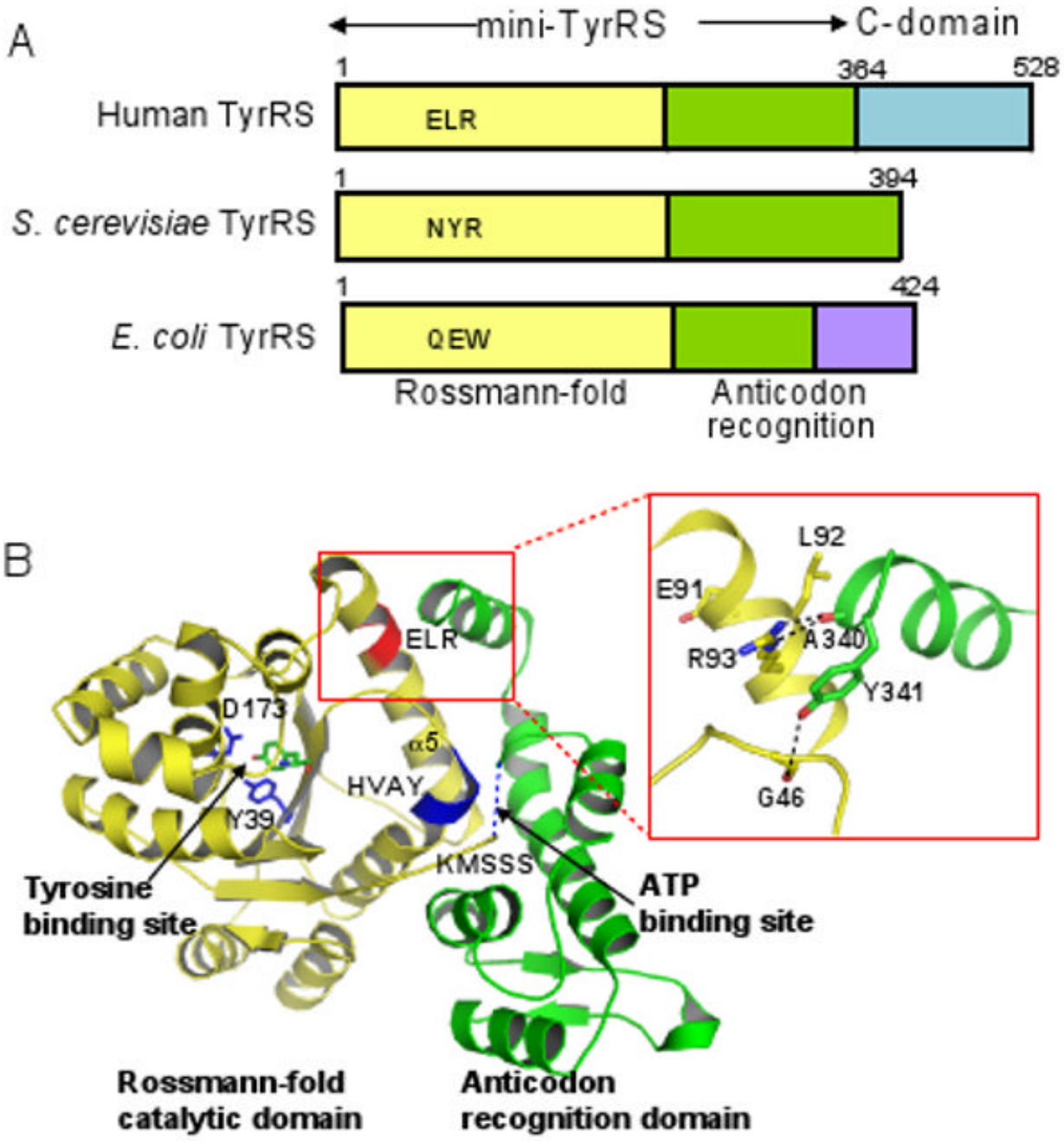

Figure 1. Domains and critical motifs in TyrRS

(A) Schematic alignment comparing human full-length TyrRS with *S. cerevisiae* and *E. coli* TyrRS. All TyrRSs have a catalytic Rossmann-fold catalytic domain (yellow) and an anticodon recognition domain (green). Human TyrRS has an extra domain (C-domain, shown in blue) appended to the C-terminal end of the anticodon recognition domain, which is not present in yeast or *E. coli* TyrRS. (*E. coli* TyrRS has a smaller C-terminal extension (purple) that is distinct from human TyrRS C-domain). The ELR motif required for cytokine activity of mini-TyrRS, is indicated in red. This motif is absent in yeast and *E. coli* TyrRS. Numbers in the schematic refer to amino acid residues.

NIH-PA Author Manuscript

NIH-PA Author Manuscript

NIH-PA Author Manuscript

(B) Structure of mini-TyrRS (PDB:1q11) indicating the location of various motifs. Removal of C-domain (not shown) from full-length TyrRS, unmasks the critical ELR motif essential for its cytokine activity. The first two domains of full-length TyrRS (Rossmann-fold catalytic domain in yellow and anticodon recognition domain in green) constitute mini-TyrRS. HVAY and KMSSS (shown as dotted lines as it is disordered in the crystal structure) motifs contribute to the formation of ATP binding site and are essential for mini-TyrRS aminoacylation activity. Tyr39 and Asp173 are required for tyrosine binding based on interactions with the bound tyrosinol in the crystal structure. ELR motif (red) is present on a surface helix (α5) and is critical for cytokine activity of mini-TyrRS. Inset shows interactions around the ELR motif. Arg93 side chain makes two hydrogen bonds with the main chain carboxyl oxygen of Ala340. The aromatic ring of Tyr341 stacks with guanidino side chain of Arg93 and its side chain hydroxyl makes a hydrogen bond with the main chain carboxyl oxygen of Gly46 present in a loop before the HVAY tetrapeptide. Both main figure and inset was generated using PyMOL (Delano, 2002).

NIH-PA Author Manuscript
NIH-PA Author Manuscript
NIH-PA Author Manuscript

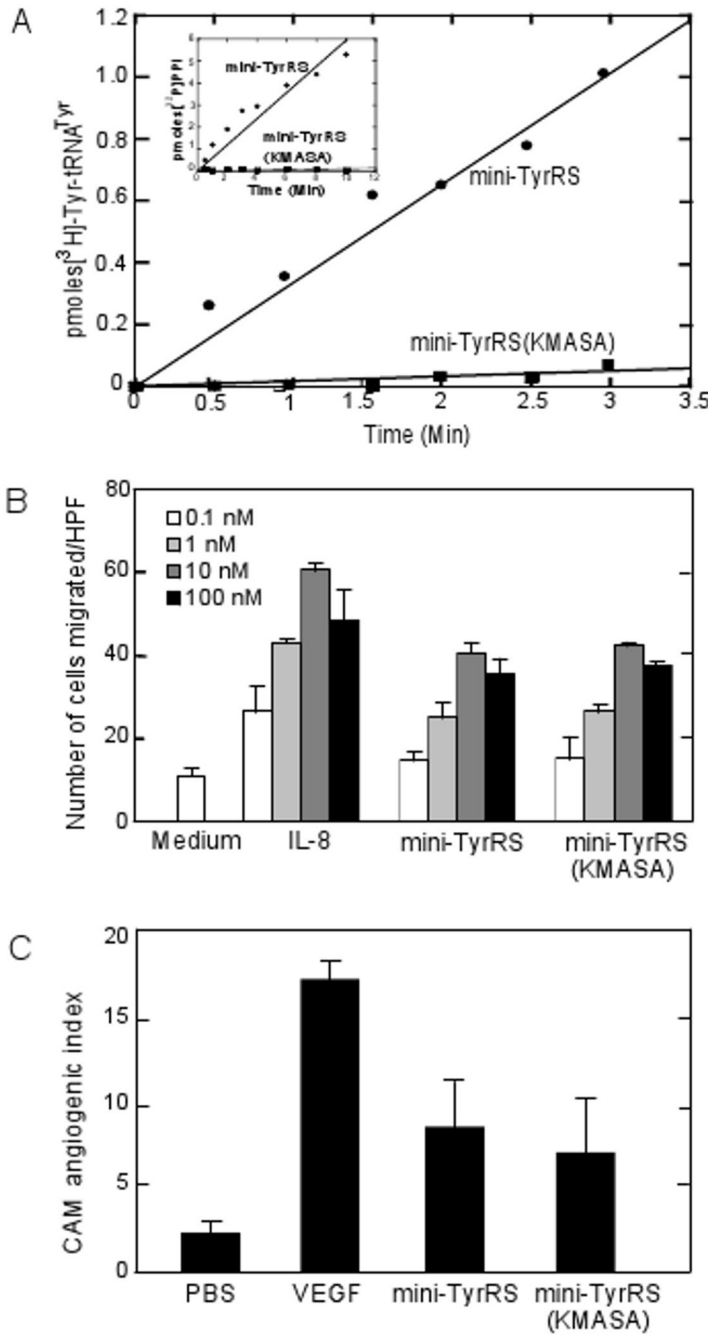

Figure 2. Mini-TyrRS catalytic variant retains cytokine functions

(A) Mini-TyrRS(KMASA) catalytic variant has significantly reduced aminoacylation activity as compared with wild-type mini-TyrRS. In each case, enzyme was tested for its ability to aminoacylate human $tRNA^{Tyr}$ with tyrosine. Mini-TyrRS(KMASA) does not catalyze the first step of aminoacylation reaction (formation of Tyr-AMP) as observed in a ATP-PPi exhange assay (Inset).

(B) Mini-TyrRS catalytic variant is active in PMN cell migration assay. Each protein or medium alone was added to the wells in the lower compartment of a chemotaxis chamber, and freshly isolated human PMNs were placed in the upper wells. The data show average number of cells per high power field (HPF) migrating in response to culture medium, IL-8, mini-TyrRS

NIH-PA Author Manuscript

NIH-PA Author Manuscript

NIH-PA Author Manuscript

and mini-TyrRS(KMASA) over a range of concentrations (0.1–100 nM). Medium indicates background, while IL-8 is the positive control. Each condition was performed in triplicate and mean ± SD is shown. The experiment was performed three times and representative data from one experiment is shown here.

(C) Mini-TyrRS catalytic variant is active in chick CAM angiogenesis assay. Collagen was copolymerized with PBS, VEGF, mini-TyrRS or mini-TyrRS(KMASA) prior to placement of the collagen implant on the chick CAM. The embryos containing the implants were incubated for a minimum of 66 hr. Blood vessels in representative implants were photographed *in vivo* through a stereomicroscope. New vessels that grow up into the implants are visualized within the grid boxes of the nylon mesh and scored as positive. The preexisting, underlying CAM vessels are out of focus and are not scored in the assay. The presence of VEGF, mini-TyrRS or mini-TyrRS(KMASA) clearly enhanced angiogenesis over the control implants (PBS treated). The data represents average of the means from multiple experiments. For both mini-TyrRS and mini-TyrRS(KMASA) p-value was less than 0.005 as compared to the control samples.

NIH-PA Author Manuscript
NIH-PA Author Manuscript
NIH-PA Author Manuscript

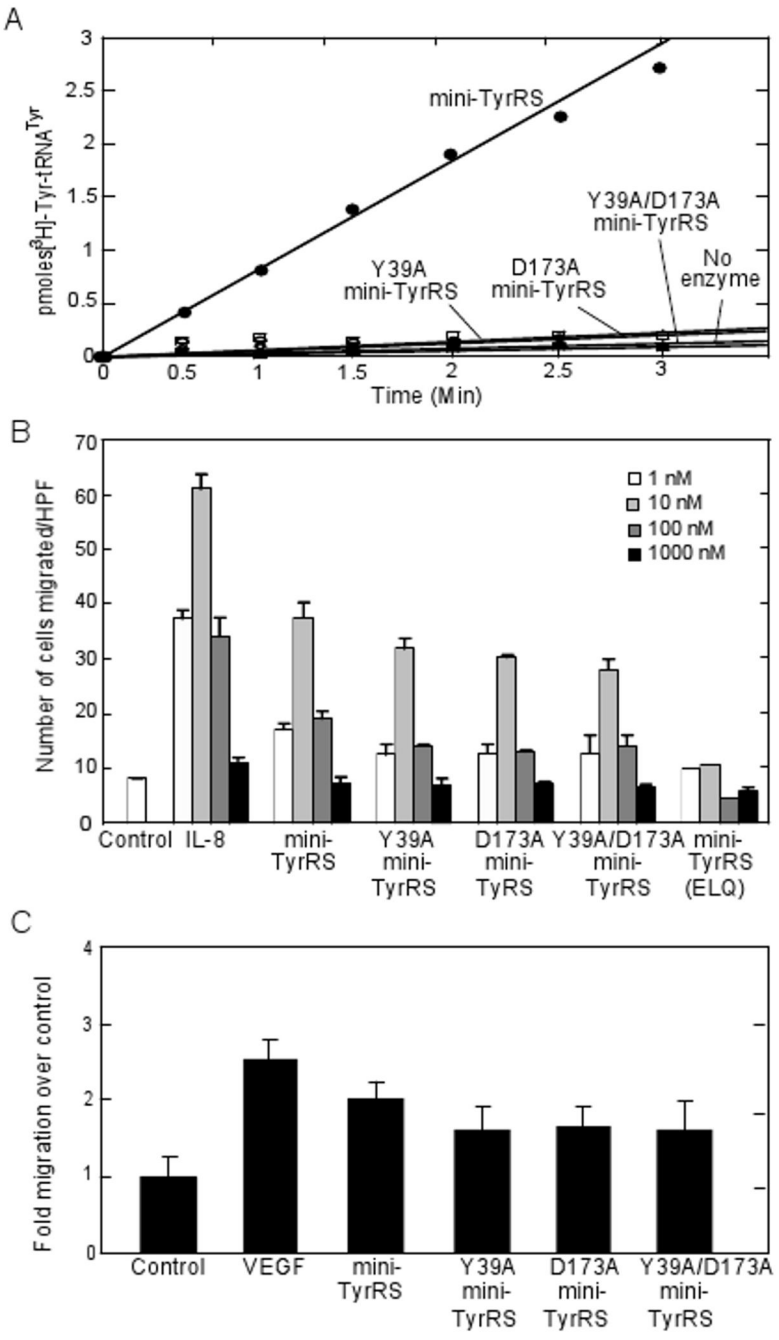

Figure 3. Mini-TyrRS tyrosine binding pocket variants retain cytokine functions

(A) Mini-TyrRS tyrosine binding pocket variants have significantly reduced aminoacylation activity. [^{3}H]Tyrosine incorporation into human tRNA^{Tyr} by 10 nM TyrRS or its variants. The three variants (Y39A, D173A and Y39A/D173A) do not show any activity in the assay.

(B) Mini-TyrRS tyrosine binding pocket variants stimulate migration of PMN cells comparable to that observed for mini-TyrRS. Protein samples (1–1000 nM) or medium alone was added to chemotaxis chamber in triplicate and mean of number of cells migrated ± SD is shown.

(C) Tyrosine binding pocket variants are active in endothelial cell migration assay. Mini-TyrRS and variants stimulated migration of HUVECs in a similar manner. VEGF was used as a

positive control. Migration of untreated monolayers was normalized to 1. Data from eight measurements was collected for each sample and mean ± SD is shown.

NIH-PA Author Manuscript
NIH-PA Author Manuscript
NIH-PA Author Manuscript

NIH-PA Author Manuscript
NIH-PA Author Manuscript
NIH-PA Author Manuscript

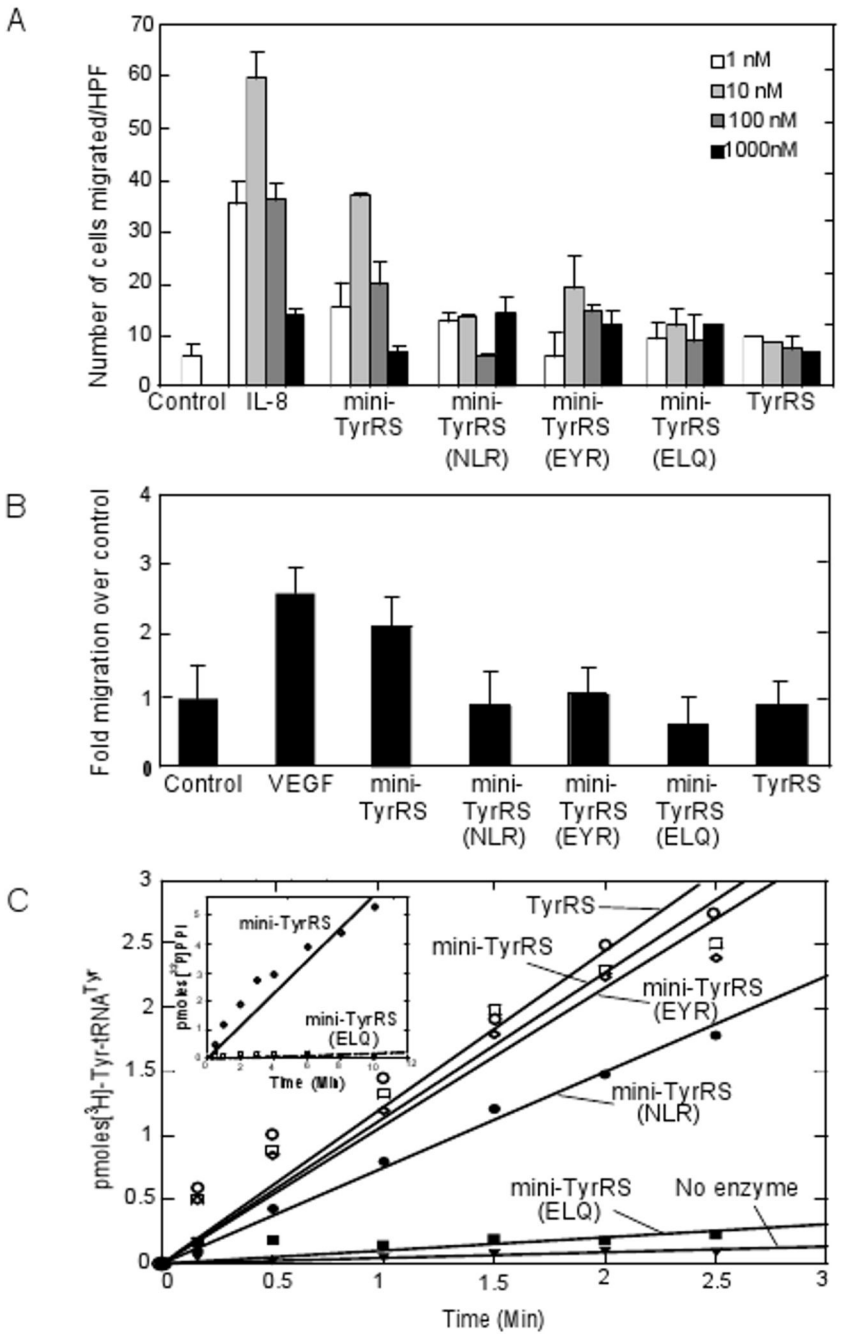

Figure 4. Mini-TyrRS ELR variants lack cytokine activities

(A) Mini-TyrRS ELR variants do not stimulate migration of PMN cells. Protein samples (1–1000 nM) or medium alone was run in triplicate and mean of number of cells migrated ± SD is shown. As control, IL-8 and mini-TyrRS induced migration of PMN cells. Mini-TyrRS (NLR) and mini-TyrRS(ELQ) or TyrRS did not stimulate migration of cells. Mini-TyrRS (EYR) had minimal cytokine activity.

(B) Mini-TyrRS ELR variants do not stimulate migration of endothelial cells. VEGF was used as a positive control. Migration of untreated monolayers was normalized to 1. Data from eight measurements was collected for each sample and mean ± SD is shown.

NIH-PA Author Manuscript

NIH-PA Author Manuscript

NIH-PA Author Manuscript

(C) Aminoacylation assays for mini-TyrRS and ELR variants. [^{3}H]Tyrosine incorporation into human tRNA^{Tyr}, as catalyzed by 10 nM TyrRS or its variants. Mini-TyrRS(EYR) variant showed activity comparable to wild-type mini-TyrRS. Mini-TyrRS(NLR) had a slight decrease in activity. Mini-TyrRS(ELQ) had significantly reduced activity. Further**,** ATP-PPi exchange assay for mini-TyrRS(ELQ) showed that it is defective in catalyzing the first step of the aminoacylation reaction (Inset).

NIH-PA Author Manuscript

NIH-PA Author Manuscript

NIH-PA Author Manuscript

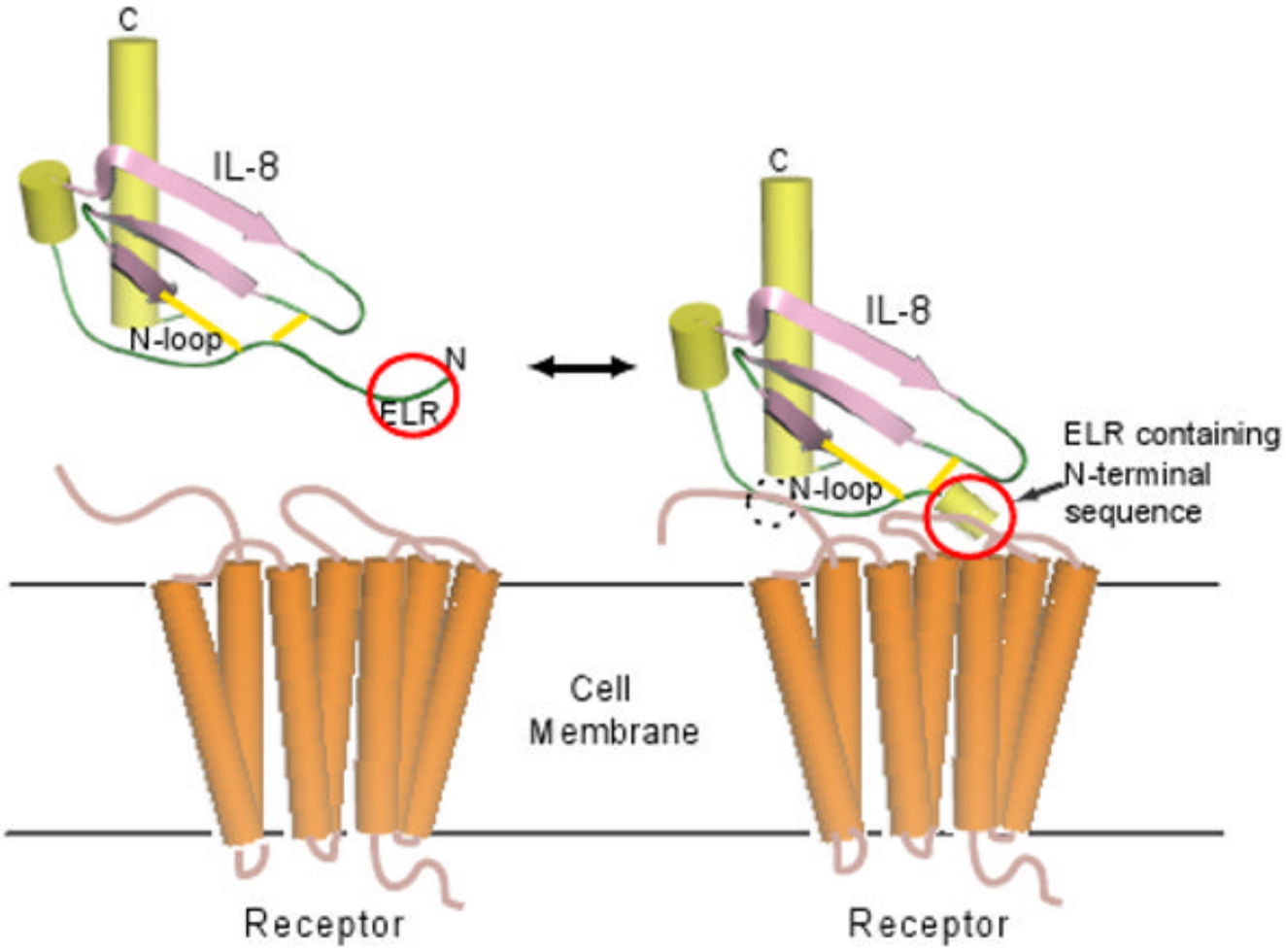

Figure 5. Hypothesis that IL-8 N-terminal sequence undergoes conformational change upon receptor binding

ELR motif preceding the first cysteine at the N-terminus is required for angiogenic activity of CXC-chemokines. In mini-TyrRS this ELR is present on a surface helix as compared to IL-8, in which it is part of a flexible loop. Thus we hypothesize that this flexible N-terminal sequence of IL-8 adopts a helical conformation upon receptor binding (shown by red circle). Conformation of unbound IL-8 was generated using PDB: 1il8, and the receptor is shown as a conceptual model. The other interacting region is shown by black dotted circle. Disulfide bonds Cys7-Cys34 and Cys9-Cys50 are shown as yellow solid lines.